

# An Automated Method for Segmenting Brain Tumors on MRI Images

A. R. Abdulraqueb<sup>1\*</sup>, W. A. Al-Haidri<sup>1</sup>, L. T. Sushkova<sup>1</sup>, M. M. Abounassif<sup>2</sup>, P. J. Parameaswari<sup>2</sup>, and M. A. Muteb<sup>2</sup>

*We present a method for segmenting images of tumors on MRI images of the brain based on an algorithm developed for automated determination of segmentation and outlining thresholds. Testing was performed by generating two databases of real MRI images of the brain, with radiology reports. Criteria for assessment of the quality of the segmentation results were: the Dice score, the Jaccard index, sensitivity, and specificity. Analysis of results obtained using this algorithm to solve the brain tumor MRI image segmentation task showed levels of sensitivity and specificity of 89% to 99%, which is evidence that assessment of the position and boundaries of brain pathology is highly effective.*

## The Task

Visualization of anatomical structures in the human body currently makes extensive use of MRI scans, which provide detailed images of different body tissues [1]. This is a widely recognized method for detecting a variety of pathologies, including brain tumors (BT).

Analysis of MRI images for the diagnosis of pathological changes in the brain requires high precision. Human vision often fails to provide for visualization of the presence of a variety of changes. Contrasting (the T1 + contrast regime) is used to increase the visualization clarity of tumor boundaries and structure in MRI scans, improving detection at early stages of disease development as a result of accumulation of contrast within tumors.

Analysis of MRI images is generally performed by radiologists manually and includes seeking and recognizing objects of interest, locating boundaries (outlining), and identifying tumor size. This is a laborious and complex task requiring a high level of training.

In many cases, segmentation techniques determine image analysis results in general, as measurements of

image object characteristics and other stages in its processing are based on the results of this procedure. This problem determines the relevance of the task of improving methods for processing MRI images and the need to develop accessory analytical tools to increase the accuracy of segmentation (extraction) of areas of pathology by automating this process.

Analysis of the literature shows that among a multiplicity of methods for segmentation of pathological changes in the brain, the most commonly used are: threshold methods, growth methods, boundary extraction method, atlas methods, and clustering methods [1-4].

As threshold methods are frequently used in image segmentation tasks, we have developed these methods for MRI image analysis on the basis of automating the procedures for determining segmentation thresholds and subsequent outlining of tumor formations with the aim of eliminating the dependence of the results on selection of the threshold and increasing the effectiveness of detecting pathological changes in the brain.

## Materials and Methods

Initial data for studying and testing the algorithm were obtained using two databases of MRI images of axial and sagittal sections obtained in the T1 + contrast regime in diagnostic investigations of patients in specialist clinics:

<sup>1</sup> A. G. and N. G. Stoletov Vladimir State University, Vladimir, Russia.

<sup>2</sup> Research Center, King Saud Medical City, Ministry of Health, Riyadh, Saudi Arabia; E-mail: atef\_alsanawy@mail.ru

\* To whom correspondence should be addressed.

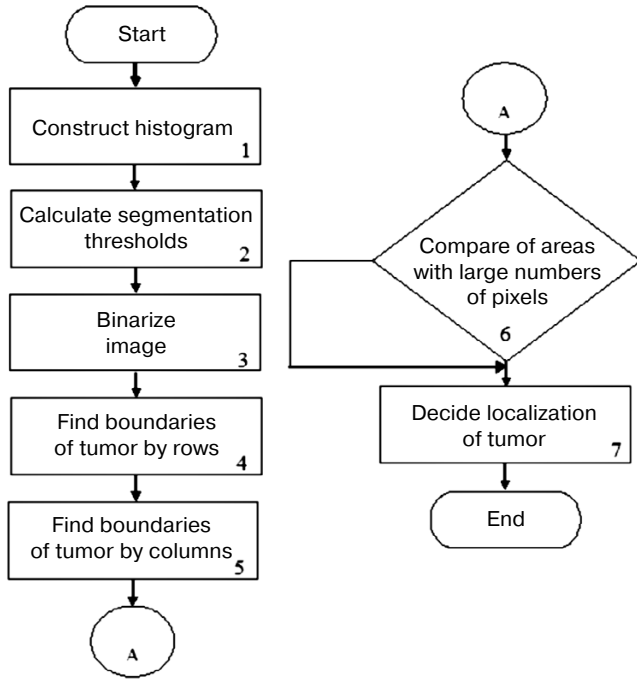


Fig. 1. Flow chart of algorithm for the method proposed here.

1) 12 images obtained in Vladimir using a Philips Intera scanner with magnetic field induction of 1.5 T;

2) 44 images obtained in Riyadh, Saudi Arabia, using a GE Signa scanner with magnetic field induction of 1.5 T.

With the aim of eliminating the dependence of segmentation results on selection of the threshold, we developed an algorithm for automated determination of the threshold on the basis of image brightness histograms. Maximum and minimum brightness threshold levels are determined, to give a range within which the tumor should be detectable. The image is then binarized using the automatically selected brightness thresholds. The resulting binary image reflects not only the target zone (the tumor), but also a number of other objects not belonging to the neoplasm, which must be removed to obtain more accurate localization of the tumor. Working from the suggestion that the tumor area is characterized by maximum brightness in rows and columns, its exact boundaries are found by calculating the mean values of pixels with maximum brightness by row and column. The flow chart scheme of this segmentation automation algorithm is shown in Fig. 1.

The segmentation automation algorithm is run in two stages.

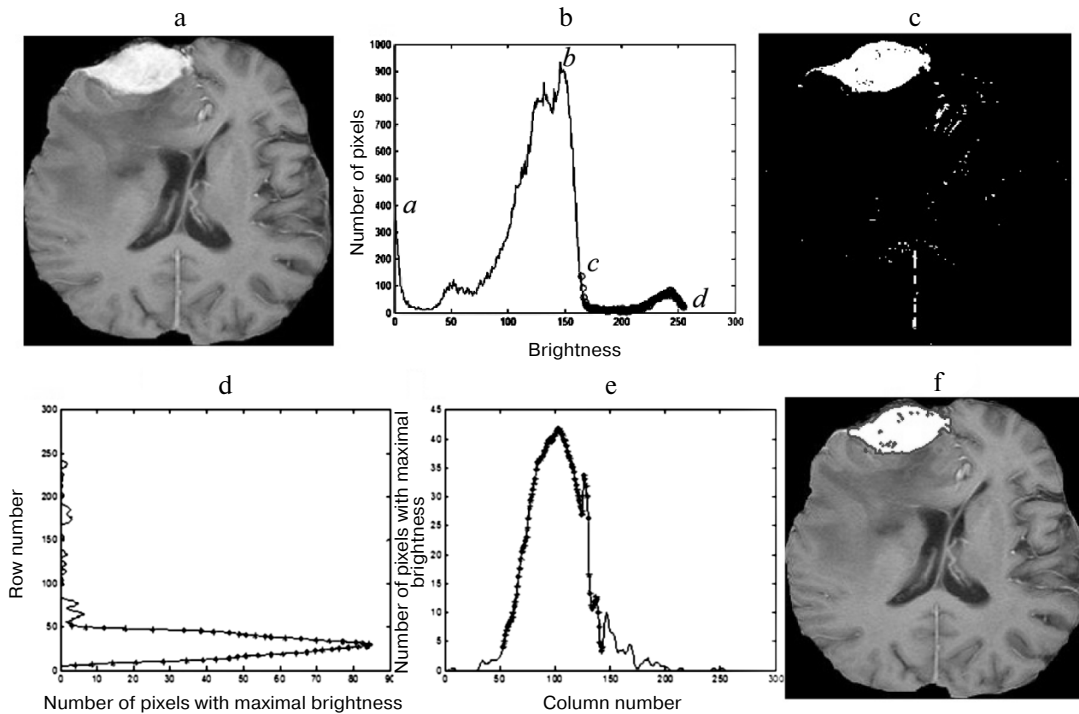


Fig. 2. Stages in the segmentation of BT on MRI brain scans.

The first stage involves automatic selection of segmentation thresholds, by constructing image brightness histograms (Fig. 1, block 1) and finding the points on this histogram corresponding to the maximum and minimum brightness intensity values within which the tumor area is located (Fig. 1, block 2).

Figure 2 shows the steps in the BT segmentation process on MRI images of the brain using an axial slice. The initial image (Fig. 2a) shows the area needing segmentation.

Figure 2 shows: the initial image (a); the processed histogram of the image with the brightness intensity values within which the tumor is located marked in circles (b); a binary image with a brightness intensity between the upper and lower limits of the brightness threshold (c); the distribution of pixels with maximum brightness by rows (d); the distribution of pixels with maximum brightness by columns (e); and the result of BT segmentation on the initial image (f). In Fig. 2b (histogram of image) the  $x$  axis shows brightness intensity values and the  $y$  axis shows the number of pixels. Here, points  $a$ ,  $b$ ,  $c$ , and  $d$  show the brightness intensity values of the image background ( $a$ ) and the gray matter ( $b$ ), as well as the lower ( $c$ ) and upper ( $d$ ) limits of the brightness threshold. In Fig. 2b, point  $a$  (first mode) characterizes a brightness intensity of zero, which corresponds to the background of the black image. The second mode (Fig. 2b) corresponds to point  $b$ , with the largest number of pixels, which characterizes the gray matter and is the reference point. The minimum brightness value of the tumor area on the right side of the second mode determines the boundary of the transition of brightness from low (gray matter) to higher, characterizing a possible boundary for the beginning of the tumor. Points  $c$  and  $d$  (Fig. 2b) characterize the lower and upper limits of the brightness threshold on the image. The outcome of the first stage of processing (Fig. 1, block 3) is the binary image (Fig. 2c). This image is characterized by pixels only

having brightness intensities between the upper (point  $d$ ) and lower (point  $c$ ) limits of the brightness threshold.

The second step consists of determining the exact boundaries of the tumor and its spatial localization in accordance with the algorithm developed for identifying the horizontal and vertical boundaries of tumors. This was done by calculating the mean values of pixels with the maximum brightness in each row (Fig. 1, block 4) and column (Fig. 1, block 5) of the image matrix. As a rule, the brain tumor localization area had maximal brightness. As shown in Fig. 2, d and e, the distributions of pixel counts by row and column in the tumor localization area had the greatest pixel values with maximum brightness. The  $x$  and  $y$  axes in Fig. 2d show, respectively, the mean values of pixels with maximal brightness and row number, while the axes in Fig. 2e shows column number on the  $x$  axis and the mean value of pixels with maximal brightness on the  $y$  axis. The plots in these figures illustrate the beginning and end of the tumor area by row (horizontal) and column (vertical). In this case, it can be seen that the tumor area is located between rows 5 and 50 and columns 54 and 150. This establishes the horizontal and vertical boundaries of the tumor, after which all points located outside the limits of the tumor are assigned the null brightness value. The result of this step of the algorithm is shown in Fig. 2f.

MRI images sometimes produce a situation in which contrast is also taken up by vessels. This leads to the result that vessels on images, like tumors, have greater intensity than other tissues (Fig. 3a). As a result, the segmentation process segments both the tumor area and the blood vessel, which is illustrated on pixel distribution plots by row and column (Fig. 3, b and c).

Figure 3 shows: the initial image (a); the distribution of pixels with maximum brightness by row (b); the distribution of pixels with maximum brightness by column (c); the initial images with the result of tumor segmentation

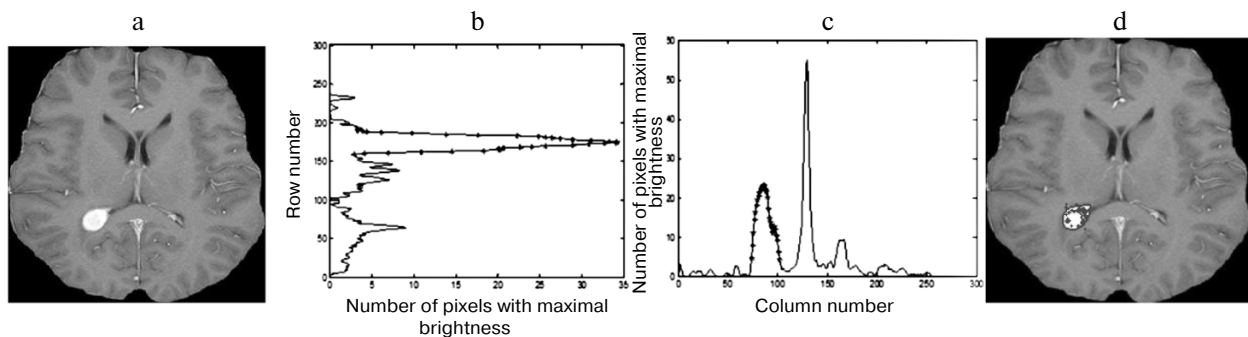


Fig. 3. Example of an image of a tumor and vessel with high brightness intensity.

**TABLE 1.** Calculated Mean Values of Criteria for Assessment of the Effectiveness of the Segmentation Algorithm Described Here

DB	$D$		$J_{ind}$		$Sens$		$Spec$	
	$M$	$\Delta$	$M$	$\Delta$	$M$	$\Delta$	$M$	$\Delta$
1	0.93	0.84-0.96	0.87	0.73-0.92	0.89	0.84-0.92	0.99	0.99-1
2	0.91	0.84-0.96	0.84	0.71-0.93	0.90	0.81-0.98	0.99	0.98-1

(d). On Fig. 3b, the  $x$  and  $y$  axes show the mean values of pixels with maximal brightness and row number respectively, while in Fig. 3b the  $x$  axis shows column number and the  $y$  axis shows the mean values of pixels with maximal brightness.

With the aim of excluding segmentation errors, tumor areas and vessels were compared with all areas with the greatest distributions of the number of pixels with maximal brightness intensities and the area with the largest number of pixels was selected (Fig. 1, block 6), as tumors generally have a larger number of pixels than vessels.

## Results

The effectiveness of the automated segmentation algorithm developed here was assessed and analyzed using a “gold standard” [5] which consisted of a solution to the segmentation task by the experimental physician (expert) using a MATLAB system.

Measures of the closeness of the segmentation results (detection) of BT with results of the gold standard were

generally recognized criteria – the Jaccard index  $J_{ind}$ , the Dice score  $D$ , the sensitivity  $Sens$ , and the specificity  $Spec$  [5, 6]. Brief descriptions of these criteria have been presented in [6].

Table 1 shows the values obtained ( $M$  is the mean,  $\Delta$  is the range) of these criteria for the effectiveness of the algorithm for the tumor segmentation task on real brain MRI images (databases: 1 – Vladimir, Russia, and 2 – Riyadh, Saudi Arabia). Analysis of these data provided evidence of the quite high effectiveness of this automated brain tumor segmentation algorithm using both the first and the second databases as examples.

For convenience, the results are presented in Fig. 4 as box plots of the Dice score, Jaccard index, sensitivity, and specificity for the first and second databases.

Analysis of these scale diagrams (Fig. 4) showed that the values of all four criteria were essentially fully grouped into the ranges  $\Delta$  shown in Table 1, which illustrates good similarity with the gold standard on images with high and low brightness intensities. The lower boundary of the values of all criteria was greater than 0.7. It is important to note that the median values for all criteria for assessing the effectiveness of this segmentation method were in the

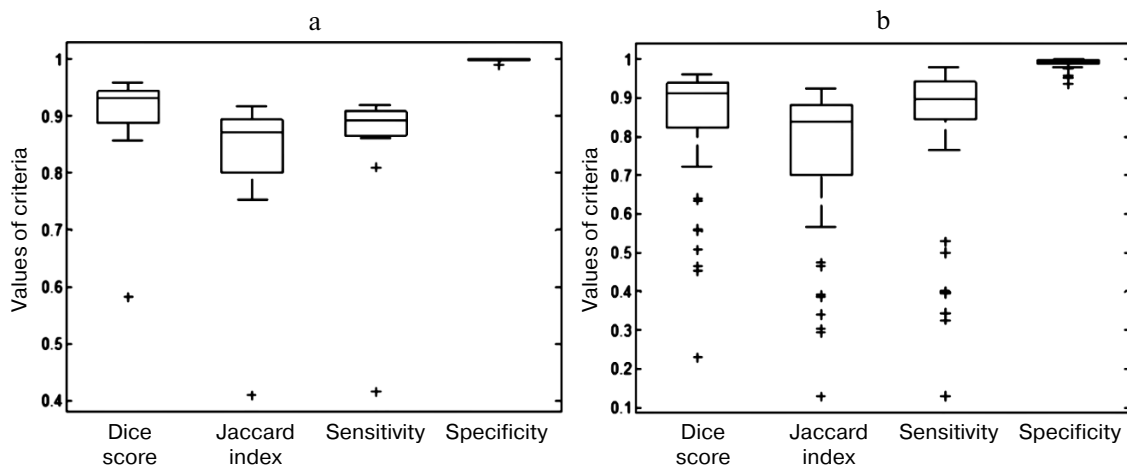


**Fig. 4.** Diagram showing the spread of values for criteria for the first (a) and second (b) databases. The  $x$  axis shows the criteria: the Dice score, the Jaccard index, sensitivity, and specificity; the  $y$  axis shows the values of these parameters.

upper quartile. The “+” symbol shows values of the criteria beyond the limits of the main ranges. These number of these can be seen to be minor.

### Conclusions

The segmentation method described here provides for automated identification of areas of pathology, with qualitative and quantitative analysis of these areas (localization, measurement of precise size and volume), which increases the diagnostic significance of MRI scan images for the physician and, as a result, the efficacy of subsequent treatment.

The result of the present studies demonstrated a quite high effectiveness for this modified automatic threshold-based segmentation method, as evidence by the levels of sensitivity and specificity of 89% to 99%.

### REFERENCES

1. Jin, L., Min, L., Jianxin, W., Fangxiang, W., Tianming, L., and Yi, P., “A survey of MRI-based brain tumor segmentation methods,” *Tsinghua Science and Technology*, **19**, No. 6, 578-595 (2014).
2. Gonzalez, R. C. and Wood, R. E., *Digital Image Processing [Russian translation]*, Tekhnosfera, Moscow (2005).
3. Anam, M., Ali, J., and Tehseen, F., “An efficient brain tumor detection algorithm using watershed and thresholding based segmentation,” *Int. J. Image Graph. Signal Process.*, No. 10, 34-39 (2012).
4. Abdulraqeb, A. R., Sushkova, L. T., and Lozovskaya, N. A., “Review of tumor segmentation methods on MRI images of the brain,” *Prikl. Zh. Uprav. Vys. Tekhnol.*, No. 1, 192-208 (2015).
5. Bjoern, M., Andras, J., Stefan, B., Jayashree, K. C., Keyvan, F., et al. “The multimodal brain tumor image segmentation benchmark (BRATS),” *IEEE Trans. Med. Imaging*, 33 (2014).
6. Abdulraqeb, A. R., Sushkova, L. T., Abounassif, M. M., Parameaswari, P. J., and Muteb, M. M., “Significance of segmentation methods in assessing brain tumor magnetic resonance images,” in: *Russian-German Conference on Biomedical Engineering* (2016), pp. 62-65.